Cation Exchange in the Presence of Oil in Porous Media

Farajzadeh, Rouhi; Guo, Hua; van Winden, Julia; Bruining, Hans

DOI
10.1021/acsearthspacechem.6b00015

Publication date
2017

Document Version
Final published version

Published in
ACS Earth and Space Chemistry

ACS EARTH AND SPACE CHEMISTRY

Article

http://pubs.acs.org/journal/aesccq

Cation Exchange in the Presence of Oil in Porous Media

R. Farajzadeh,*[,†,‡] H. Guo,[‡] J. van Winden,[†] and J. Bruining[‡]

[†]Shell Global Solutions International, 2288 GS Rijswijk, The Netherlands

[‡]Delft University of Technology, 2628 CD Delft, The Netherlands

ABSTRACT: Cation exchange is an interfacial process during which cations on a clay surface are replaced by other cations. This study investigates the effect of oil type and composition on cation exchange on rock surfaces, relevant for a variety of oil-recovery processes. We perform experiments in which brine with a different composition than that of the in situ brine is injected into cores with and without remaining oil saturation. The cation-exchange capacity (CEC) of the rocks was calculated using PHREEQC software (coupled to a multipurpose transport simulator) with the ionic composition of the effluent histories as input parameters. We observe that in the presence of crude oil, ion exchange is a kinetically controlled process and its rate depends on residence time of the oil in the pore, the temperature, and kinetic rate of adsorption of the polar groups on the rock surface. The cation-exchange process occurs in two stages during two phase flow in porous media. Initially, the charged sites of the internal surface of the clays establish a new equilibrium by exchanging cations with the aqueous phase. At later stages, the components of the aqueous and oleic phases compete for the charged sites on the external surface or edges of the clays. When there is sufficient time for crude oil to interact with the rock (i.e., when the core is aged with crude oil), a fraction of the charged sites are neutralized by the charged components stemming from crude oil. Moreover, the positively charged calcite and dolomite surfaces (at the prevailing pH environment of our experiments) are covered with the negatively charged components of the crude oil and therefore less mineral dissolution takes place when oil is present in porous media.

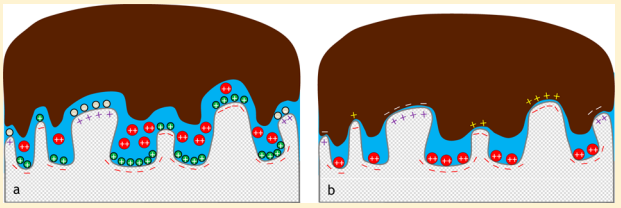

KEYWORDS: *Cation exchange, Wettability, Rock-fluid interaction, Wetting film, Heterogeneous charge, Clays, Geochemistry*

1. INTRODUCTION

The efficiency of improved or enhanced oil recovery (IOR/EOR) processes is often influenced by the composition of the flowing aqueous phase and is thus affected by the mass exchange between fluid and solid phases. For example, the rheology of polymers or the magnitude of the interfacial-tension reduction by surfactants strongly depends on the ionic strength and hardness (concentration of divalent cations) of the aqueous phase.[1,2] In recent years, the additional oil extracted by tuning the composition of the injected water has revived the interest in a more detailed understanding of the nature of the interactions between the rock and the fluids residing in the pore.[3−18]

Several interfacial phenomena occur simultaneously during two-phase flow in porous media, the extent of which depends on the compositions of the flowing (aqueous and oleic) and the stationary (rock) phases and the contact area affected by the surface roughness or irregularities. Indeed, reservoir rocks consist of irregularly shaped pores and grain assemblages with sharp edges and corners.[19] The asperities and sharp edges are the "pinning points" at which crude oil contacts the rock[20−23] possibly with a very thin water film in between held together by molecular forces on the surface.[23−30] On other surfaces, such as quartz, the oil is separated from the rock by a "thicker" non-uniform water film.[19] The stability of the water films depends on the equilibrium between interaction of double layer forces and van der Waals forces.[25,29] A double layer occurs when a charged surface is in contact with an aqueous phase. The ions with an opposite charge will have a higher concentration than the bulk concentration near the surface, whereas ions with a charge of the same sign will have a concentration less than the bulk concentration near the surface. When the oil−water surface and the rock−water surface have the same sign, it can be shown that the double layers repel each other, which is conducive to a stable water layer. The presence of high salt concentrations shields the surface charges leading to a reduced double-layer repulsion.[29−31] The Debye length, κ^{-1} [m] is the characteristic distance over which a charge is shielded by the ions in a solution and is given by[31]

$$\kappa^{-1} = \sqrt{\frac{\epsilon_r \epsilon_0 k_B T}{2 N_A e^2 I}} = 9.63 \times 10^{-9} \sqrt{\frac{1}{I}} \quad (1)$$

where $I = \Sigma\ 1/2\ c_i z_i^2$ is the ionic strength [mol/m^3], ε_r (20 °C) = 80.1 [-] is the relative permittivity, $\varepsilon_0 = 8.854 \times 10^{-12}$ [F/m = C^2/J/m] is the permittivity of free space, $k_B = 1.38 \times 10^{-23}$ [J/K] is the Boltzmann constant, $N_A = 6.0225 \times 10^{23}$ is Avogadro's number, and $e = 1.602 \times 10^{-23}$ C is the charge of an electron. In the case of the presence of a water film, van der Waals forces are generally attractive because the dielectric coefficient of water exceeds that for rock and oil and

Received: December 21, 2016
Revised: March 14, 2017
Accepted: March 16, 2017
Published: March 16, 2017

DOI: 10.1021/acsearthspacechem.6b00015
ACS Earth Space Chem. 2017, 1, 101−112

because the refractive index of water is generally less than for rock and oil (see Figure 1). These two forces suffice if the thickness of the water film considerably exceeds the molecular size or surface roughness; otherwise structural forces have to be considered. The force per unit surface area is called the disjoining pressure. If the capillary pressure is less than the local maximum disjoining pressure at large film thickness, the water film is stable. The surface charge can be calculated by considering the relevant chemical surface complexation reactions[23,32−34] and can be found using PHREEQC.[35]

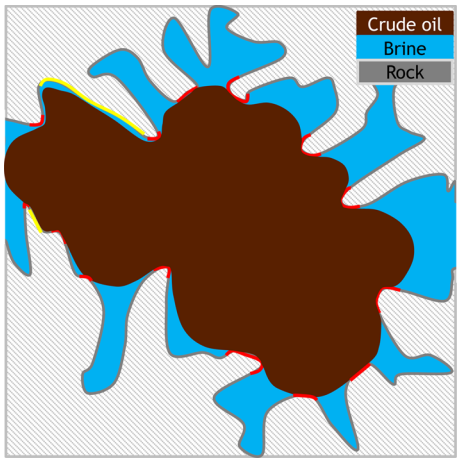

Figure 1. Schematic of an oil drop inside irregular pores. The red lines represent the "pinning points"[20] or "welding spots",[24] that is, charged mineral edges and asperities where oil can directly contact rock (in the presence of a hydration layer). The yellow lines represent the quartz surface and the silica-like surface of clays on which a thick nonuniform water film separates oil from the rock surface.

The charge of the oil−water surface is determined by the presence (or more strictly ionization) of functional groups such as carboxylic acids (negative charge) and basic compounds such as pyridines and quinolones (positive charge) at a given pH.[28] A larger part of the rock surface is covered with a water film of variable thickness, depending on the ionic strength and pH of the flowing solution; however, some "asperities" will stick out of the water layer into the crude oil. The diffusion of polar components of the crude oil into the water film may lead to direct contact of oil with the rock and alteration of the wetting state of the surface similar to "spot-welding".[20−22] Depending on the nature of the charges on the rock surface (mineral type) and components of the crude oil and water, oil can be attached to the rock surface through several mechanisms such as ligand exchange, cation bridging, anion and cation exchanges, hydrogen bonding, van der Waals interaction, and so forth.[7] These mechanisms require polar groups in the crude oil and their relative contribution depends on the composition of the phases; in particular, the composition of the aqueous phase is strongly affected by the geochemical reactions.

Cation exchange is an interfacial process during which a cation on, for instance, a clay surface is replaced by another cation. The capacity of the rocks to retain cations is measured by the cation-exchange capacity (CEC), which is the sum of the quantity of positive charges (cations) neutralizing permanent and variable pH-dependent charges. The CEC strongly depends on the rock mineralogy, the surface area, and charge and size of the ion.[36−39] Under steady-state chemical conditions, the composition of a cation exchanger is in equilibrium with the formation brine. When the composition of the brine is altered, the cation exchanger readjusts its composition to a new equilibrium with the injected brine. The exchanger acts as a temporary buffer and may alter the brine composition through a process known as ion chromatography.[40−42] If the resulting salinity is too high or the capillary pressure is high,[29] the water film covering the rock surface becomes unstable resulting in a direct contact of oil with the rock surface (albeit often in presence on a thin hydration layer). On the other hand, if the salinity is low dominance of repulsive forces results in expansion of the double layer and eventually stabilizes the water films on the rock surface. If salinity becomes too low, simultaneous effects of (viscous) drag and electrostatic forces mobilize some fines and/or deflocculate clays (interlayer forces between clay layers that control the swelling state and integrity are mainly electrostatic interactions), which might be entrapped and block the rock pores.[14−17] The charge density and distribution on the alumina-like surfaces of the clay also varies because of the cation-exchange reactions.

The effect of cation exchange on oil recovery was first applied to surfactant flooding[43−45] and has been since considered as an important component of the chemical enhanced-oil-recovery processes.[46−50] Lager et al.[7] argued that the cation exchange between the mineral surface and the invading brine can desorb oil from the rock surface.

Despite its relevance, the effect of oil on cation exchange has not been carefully studied. Most of the knowledge on this topic is inferred from indirect measurements such as the amount of produced oil (in the case of low-salinity-water flooding) or delays in breakthrough of the injected alkali (in the case of alkali-surfactant−polymer flooding).[47,51] All the experiments on this topic have been exclusively conducted without crude oil. However, as we will show in this study, the presence of oil and the dynamics of the interactions between the crude oil, brine, and the rock can lead to different results than those inferred from the single-phase experiments. This can in return pose questions to the direct translation of the coreflood experiments to field-scale water- or chemical-flooding projects. We hypothesize that (1) adsorption of basic components of the crude oil on the cation exchange sites reduces the cation exchange capacity of the rock, and (2) adsorption of acidic components of the crude oil on the calcite and dolomite inhibits the dissolution of these minerals at elevated temperatures. It is therefore our objective to investigate the effect of the oil type and composition on the extent and nature rock-fluid interactions in porous media. We perform experiments in which brine with a different composition than that of brine initially in the cores is injected into these cores with and without the remaining oil saturation. The CEC of the rocks was calculated using the ionic composition of the effluent histories. Single-phase experiments were conducted to obtain the cation-exchange capacity of the cores, denoted by Q_v (mequiv/mL pore volume), in the absence of the oil. The two-phase experiments were conducted with and without aging the cores with crude oil. When the cores were not aged at room temperature, the effect of oil on the CEC was insignificant; however, at a higher temperature the polar components of the oil started to interact with the oil. A kinetic behavior was observed for this process. This was confirmed by the reduced CEC of the core that was aged with the crude oil. In this case, because the oil was in contact with the rock for a longer period, the positively charged components of the oil exchanged with the cations adsorbed on the rock. The structure of the paper is

DOI: 10.1021/acsearthspacechem.6b00015
ACS Earth Space Chem. 2017, 1, 101−112

as follows. In Section 2, we briefly present the reactions considered in this study. Next, we describe the experimental material, setup, and procedure in Section 3. In Section 4, the results of the experiments and their interpretations are discussed. We end the paper with the main conclusions of this study.

2. CALCULATION OF CATION EXCHANGE CAPACITY

In the simulations, we consider two main geochemical reactions, namely, cation exchange and dissolution of dolomite and calcite. The simulations were performed using Shell's in-house transport simulator, MoReS,[52] which is coupled to the chemistry package PHREEQC.[47,53] PHREEQC is a software program with an extensive and editable database (with chemical reactions and their equilibrium constants) and can simulate chemical reactions to provide the composition of the aqueous phase in contact with minerals, gases, exchangers, and sorption surfaces.[35] The default phreeqc.dat database file was included in our calculations, which uses Davies or Debye−Hückel equations for charged species.

To model the ion exchange the amount of exchanger, denoted by X (= Q_v, mequiv/mL of pore volume) and defined as master exchange species in the PHREEQC database, should be provided. The ion exchange reactions occur in two steps in PHREEQC, which uses mass-action expressions based on half-reactions between the aqueous species and a fictive unoccupied exchange site[41] for each exchanger. The following exchange reactions were modeled in this study

$$Na^+ + X = NaX \quad K_{Na} = \frac{[NaX]}{[Na^+][X]} \tag{2}$$

$$Ca^{2+} + 2X = CaX_2 \quad K_{Ca} = \frac{[CaX_2]}{[Ca^{2+}][X]^2} \tag{3}$$

$$Mg^{2+} + 2X = MgX_2 \quad K_{Mg} = \frac{[MgX_2]}{[Mg^{2+}][X]^2} \tag{4}$$

The combination of eq 2 with eq 3 and eq 4 provides the reactions that are more commonly used for modeling the exchange of sodium, calcium and magnesium ions

$$2NaX + Ca^{2+} = CaX_2 + 2Na^+ \quad K_{Ca/Na} = \frac{[CaX_2][Na^+]^2}{[Ca^{2+}][NaX]^2} \tag{5}$$

$$2NaX + Mg^{2+} = MgX_2 + 2Na^+ \quad K_{Mg/Na} = \frac{[MgX_2][Na^+]^2}{[Mg^{2+}][NaX]^2} \tag{6}$$

where $K_{Ca/Na} = K_{Ca}/K_{Na}^2$ and $K_{Mg/Na} = K_{Mg}/K_{Na}^2$. In the simulations, we used $\log_{10} K_{Na} = 0.0$, $\log_{10} K_{Ca} = 0.77$,[54] and $\log_{10} K_{mg} = 0.60$.[55] Another important equation is the charge-balance equation, which sets the sum of the equivalent anions and cations, including those on the rock surface, to zero.

We use the measured concentrations of the ions in the first effluent as the initial concentrations of the respective ions in the simulations. The measured concentrations of the injected low-salinity brine were used as boundary condition, which were slightly different from the reported concentrations in Table 1 due to small variations in preparing the various solutions. We neglected the role of proton exchange in competition for exchange sites, which is justified because the pH variations were not large, as can be observed in the experimental results.

Table 1. Compositions of High-Salinity and Low-Salinity Brines (in mmol/L and mequiv/L)

	high-salinity brine (HSB)		low-salinity brine (LSB)	
component/description	mmol/L	mequiv/L	mmol/L	mequiv/L
Na^+	217	217	35.5	35.5
Ca^{2+}	1.8	3.6	2.55	5.1
Mg^{2+}	1.35	2.7	0.775	1.55
Cl^-	223.2	223.2	42.15	42.15
solution normality [N]		223.3		42.15
fraction of divalents, [f_{2+}]		0.03		0.16
total divalent concentrations	3.15	6.3	3.325	6.65
ionic strength	275 mmol/L		136 mmol/L	
Debye screening length	20.4 nm		26.4 nm	

For larger pH variations (±0.5) hydrogen exchange should be considered. The chloride ion (Cl^-) was used as the buffer to satisfy the charge balance errors and compensate for the anions that were not considered in our calculations. Moreover, dissolution of calcite and dolomite was considered in the calculations.

3. EXPERIMENTS

3.1. Chemicals. The brine used in the experiments was prepared by dissolving NaCl, $MgCl_2{\cdot}6H_2O$, and $CaCl_2{\cdot}2H_2O$ (Fisher Scientific) in deionized water. The compositions of the high-salinity and low-salinity brines are shown in Table 1. The properties of the crude oils are listed in Table 2.

3.2. Core Samples. Berea sandstone cores were used to perform the experiments. The bulk mineral composition of Berea sandstone[56,57] was characterized by XRD, the results of which are shown in Table 3. The geochemical reactions occur at the surface of the rock (and in particular clays because of their large surface area)[36−39] and therefore bulk mineralogy is only a partial indicator of the presence of minerals that might influence the direction of the reactions.

The cores had a diameter of 3.8 cm and length of 17.0 cm. The permeability and porosity of the cores were about 80−120mD and 0.20 ± 0.1, respectively. The cores were cast in Araldite self-hardening glue to avoid production from the axial core sides. After hardening, the glue was machined so that the core fitted precisely in the core holder. One hole was drilled through the glue layer to the core surface to allow pressure measurements. The core-holder is made of poly(ethylene ether ketone) (PEEK).[58−60]

In our discussions, we will interchangeably use the terms "external" and "edge" surfaces whose charges are pH dependent. These charges occur on the clay edges because of the protonation/deprotonation of the surface hydroxyl groups and therefore may vary with the pH.[61] Moreover, we use the terms "internal surface", "basal surface", and "faces" to refer to the sites with the permanent charges on the clay surfaces. These charges occur because of the isomorphous substitution of the cations with a larger valence by the cations with a smaller valence resulting in a net negative charge. Table 4 provides a summary of the main attributes of the clay surfaces.

3.3. Experimental Setup. The experimental setup is shown schematically in Figure 2. A P500 pump was used for injection of brine. A transfer vessel connected to another pump was used to inject crude oil into the core. The pressure transducers monitored the pressure-drop over the inlet and outlet. A backpressure regulator was mounted to set the outlet

DOI: 10.1021/acsearthspacechem.6b00015
ACS Earth Space Chem. 2017, 1, 101−112

Table 2. Properties of the Crude Oils Used in the Experiments[a]

oil property	IFT with FW	API	density	viscosity	density	viscosity	TBN	TAN
unit	[mN/m]	[°API]	[g/cm3] (20 °C)	[mPa.s] (20 °C)	[g/cm3] (60 °C)	mPa·s (60 °C)	[mg KOH/g oil]	[mg KOH/g oil]
crude oil A	30	34.2	0.8540	4.7765	0.8153	3.8216	0.90	0.15
crude oil B	27	41.6	0.8176	3.2769	0.7911	1.6755	<0.1	0.17

[a]IFT, TBN, and TAN stand for interfacial tension, total base number, and total acid number, respectively.

Table 3. Mineralogical Composition (Mass Fraction, wt %) of the Berea Sandstone Used in the Experiments[a]

quartz	dolomite	calcite	illite/mica	kaolinite/chlorite	albite	orthoclase	siderite
94.9	1.1	0.2	0.40	1.6	0.2	1.3	0.5
clay fraction			50.6	40.4 (Kaol)/9 (Chlorite)			
CEC (cmol/kg)			10−40	1−15			
surface area (m^2/g)			80−150	5−20			

[a]The numbers in the brackets are the clay fraction of the rock.

Table 4. Clays Surfaces and Their Main Attributes

term	charge type
faces, internal or basal surfaces	Permanent charge due to isomorphous substitution of, for instance, Si^{4+} by Al^{3+}. The net charge of the internal surface of the clays is negative. The internal surfaces will not come in contact with oil.
edges or external surfaces	Both positive and negative charges may exist at the edges.[61] These charges are pH dependent. The oil will come in contact with the external surface of the clays.

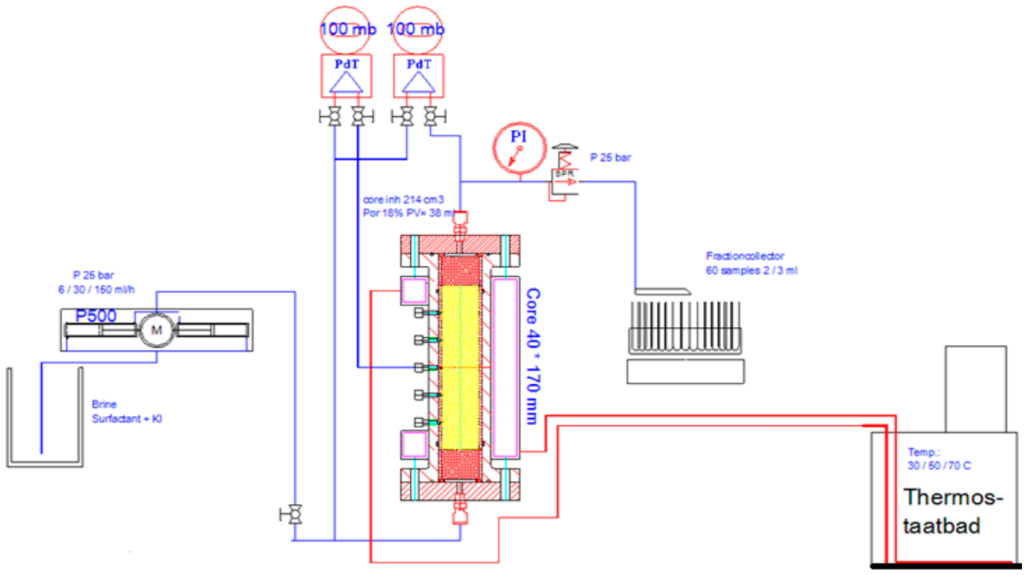

Figure 2. Schematic of the setup used in the core-flow experiments. It consists of a coreholder in which a core is mounted. The core is kept at a constant temperature using a thermostat bath. The pressure is kept constant using a homemade back-pressure regulator.

pressure during the experiment. An in-house data acquisition system was used to record the pressures. The produced fluids were collected using a fractional collector. Water from a thermostated bath was circulated through a sleeve around the core-holder to keep the core at a desired constant temperature[20−60] °C. An oven was used to set a constant temperature in experiments.[7−9]

3.4. Experimental Procedure. The leakage-proof setup was flushed with CO_2 at atmospheric pressure to remove air from the system and then vacuumed for 12 h to remove the CO_2. Next, at least 20 pore volumes of high-salinity brine (HSB) were injected with increasing pressure steps of 5 bar to a maximum pressure of 20 bar to dissolve and remove the remaining traces of CO_2 and fully saturate the core with brine. All the fluids were injected with a rate corresponding to an interstitial velocity of 1 ft/d. The permeability of the core was also measured by changing the injection rates. In the single-phase experiments, the low-salinity brine was injected after this step and the effluent was collected at intervals of 5 min to measure its ionic composition using the inductively coupled plasma mass spectroscopy (ICP) technique. In the two-phase experiments, after conducting the single-phase part of the experiment, (1) the core was flushed with the high-salinity brine to reestablish the initial condition similar to the single-phase stage,; (2) the core was saturated with the crude oil with an injection rate of 1−4 mL/min until no water production was observed at the outlet and the pressure remained constant; (3) the high-salinity brine was injected to produce the mobile oil; and (4) the low-salinity brine was injected to study the effect of the remaining oil on the cation exchange. In Exp. 6, the

DOI: 10.1021/acsearthspacechem.6b00015
ACS Earth Space Chem. 2017, 1, 101−112

setup was shut down after step 3 to age the core at a temperature of 60 °C and 20 bar for 8 weeks.

4. RESULTS AND DISCUSSION

4.1. Exp.1: Single Phase Core Flow. Two single-phase experiments were conducted to determine the cation-exchange capacity of the Berea rock samples using PHREEQC as the base case. The results of these two experiments were similar and therefore only one experiment is reported here.

Figure A.1 in Appendix A shows the history of the concentration of $Na^+/Ca^{2+}/Mg^{2+}/Cl^-$ ions and the measured pH values of the effluents during injection of the HSB into the core. The pH and the concentration of the measured ions slightly decrease and attain values of the injected brine concentration. There is no evidence that significant cation exchange occurs during this process.

Figure 3 shows the effluent concentrations after injection of low-salinity brine (LSB) into a core initially saturated with

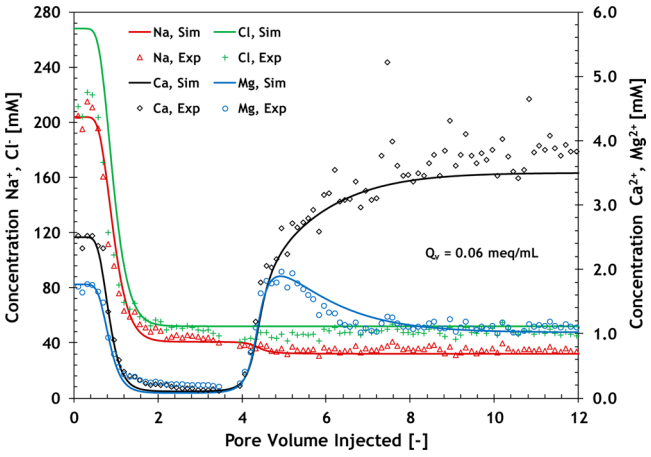

Figure 3. Production history of the effluents obtained from the ICP measurement during low-salinity brine injection in Exp. 1 (no oil present in the core). PHREEQC model calculations are compared with the experimental data using Q_v = 0.06 mequiv/mL and dispersivity length of 0.85 mm. Symbols indicate measured concentrations and lines are calculated using the PHREEQC model.

high-salinity brine. For three cations ($Na^+/Ca^{2+}/Mg^{2+}$), between injection and production points there are three regions separated by a low-salinity front (an indifferent wave) and a salinity shock, that is, a steep change of salinity. From upstream to downstream there is a region where the composition is in equilibrium with the initial concentration (HSB), then a region with an intermediate composition, which is the result of the cation stripping, and finally a region where the composition is slightly higher than the composition of the injected LSB.[43−45] The anion (Cl^-) travels with no significant retardation interaction (no retention) as its breakthrough occurs after about one pore volume (PV). The injected cations exchange with the clay and consequently their breakthrough is retarded. The presence of dispersion is apparent from the shape of the first front in our experiments, that is, the change from the initial salinity to the intermediate salinity occurs in a gradual manner because of the dispersive and diffusive mixing of the fluids. The spreading of the front in the experiments is most likely due to mixing caused by the presence of small-scale heterogeneities in the core. The calculation obtained from the PHREEQC model is in good agreement with the experimental data, where we use Q_v = 0.06 mequiv/mL PV and a dispersivity length of 0.85 cm as input parameters. The calculated solution is obtained without considering the dissolution reactions. Figure 4 shows

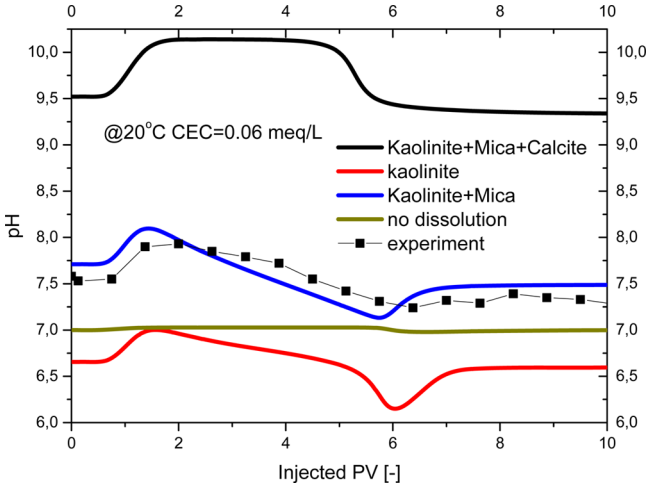

Figure 4. Simulation results of the measured pH during Exp. 1 (no oil present in the core) with different rock compositions.

the measured pH values from the effluent at atmospheric conditions. Neglecting the dissolution, the pH value determined from PHREEQC is not the same as in the experiments, which shows a similar trend but the acidity is 0.5 pH units larger than the computed value with PHREEQC. Possible reasons are that the surface composition of Berea sandstone differs significantly from the bulk composition and/or there are some minerals that are undetected by XRD. Moreover, desorption of protons (H^+) due to the presence of calcium and magnesium oxides could be another reason for a lower calculated pH than observed in the calcite dissolution case.[62] The dissolution of CO_2 from air during measurements could be another reason for the low observed pH value. The pH can be matched by varying the surface composition, however, with no clear justification. We only present the results of the pH measurements in Appendix A to allow a more sophisticated future interpretation because our focus is on region II and the results of which are not much affected by dissolution/precipitation reactions.[45]

4.2. Exp. 2: Effect of Injection Rate on Cation Exchange. To examine the effect of flow rate on the cation exchange, we performed Exp. 2 at two different flow rates (1 ft/day and 3 ft/day). A single core was used to conduct these experiments. To check the reversibility of the cation exchange process, we carried out an experiment with the sequence of HSB to LSB then again HSB to LSB. Histories of each ion collected in the effluent (Figure 5) and the pH values (Figure A.2a) in the two LSB injection processes show that within the range we investigated and during single-phase flow cation-exchange reactions are not dependent on the flow rate. The results have also been simulated with PHREEQC, using a dispersivity value of 0.85 cm and Q_v = 0.06 mequiv/mL. Experimental data points obtained for the two different flow rates coincide with each other but deviate from the model predictions with PHREEQC. A further study is needed with a wider range of flow rates to observe the kinetic effect on the cation-exchange process. However, for the range of velocities inside oil reservoirs (away from wells) we expect that for a field time scale cation exchange reactions are "instantaneous" and equilibrium models will be sufficient to simulate the behavior.

DOI: 10.1021/acsearthspacechem.6b00015
ACS Earth Space Chem. 2017, 1, 101−112

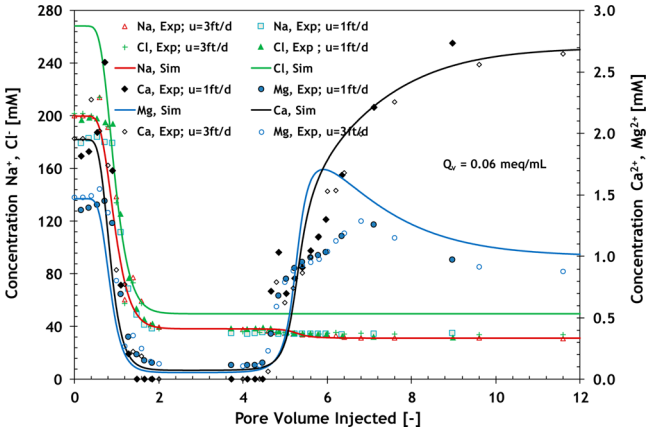

Figure 5. Flow-rate dependency of the cation exchange process in Exp. 2 (single phase with 3 ft/day injection velocity). Symbols indicate measured concentrations and lines are results from the model.

4.3. Exp. 3: Temperature Effect on the Cation Exchange.

To investigate the effect of temperature on cation exchange we carried out Exp. 3, in which the temperature was raised from 20 °C (Exp. 3a) to 60 °C (Exp. 3b). Figures 6 and 7

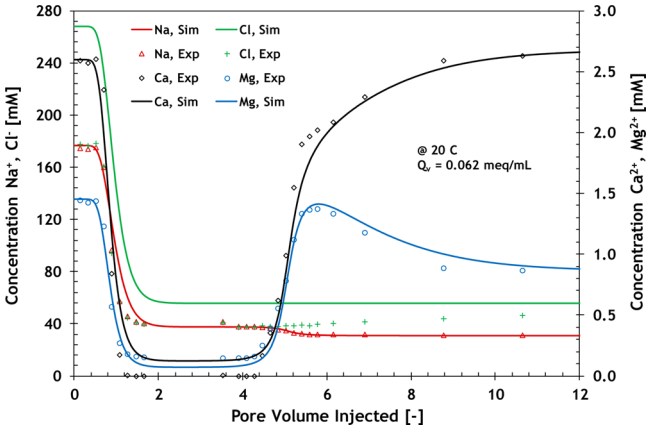

Figure 6. History of concentrations of effluent ions in Exp. 3a (no oil present in the core) at T = 20 °C. Symbols indicate measured concentration, lines are modeled.

show the concentrations of the ions determined from the effluent in Exp. 3a and 3b during LSB injection, respectively. The concentrations of Mg^{2+} and Ca^{2+} after the retardation front in Exp. 3b are higher than those in Exp. 3a, because of the higher dissolution rate of dolomite and possibly calcite at higher temperatures.[63] This is confirmed by the higher pH values of the effluents in Exp. 3b compared to Exp. 3a (Figure A.2b). The pH value increases by 1.2 pH units from 7.2 in Exp. 3a to 8.4 in Exp. 3b.

Exp. 3a can be simulated using a Q_v of 0.062 mequiv/mL. Because no dissolution was observed in the experiments, dissolution reactions were not included in simulating Exp. 3a. However, in Exp. 3b inclusion of the dissolution reactions (mainly dolomite) was necessary because of the higher rate of dissolution at 60 °C. With no dissolution reactions the data at 60 °C can be fitted to the model with a Q_v value of 0.055 mequiv/mL (dashed line in Figure 7 for Mg^{2+}). However, this match is not considered to have physical meaning because it implies that in contrast to expectation the total number of surface sites increases with increasing temperature.[64−66]

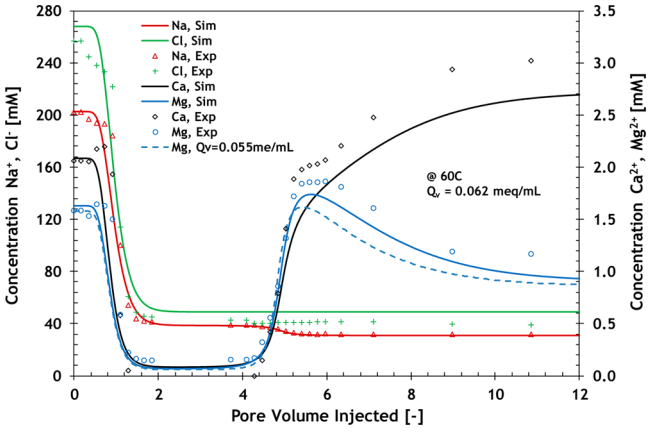

Figure 7. History of concentrations of effluent ions in Exp. 3b (no oil present in the core) at T = 60 °C. Symbols indicate measured concentration, lines are modeled. The CEC remains constant within the range of temperature investigated in this study.

The attachment of the ions on the rock surface occurs on the pre-existing charged surfaces. The charge distribution of the surface can be determined using streaming potential or zeta potential measurements. In particular, Reppert and Morgan[66] found that the magnitude of the zeta potential for Berea sandstone in contact with brines containing NaCl slightly increases as the temperature increases (0.044 mV/°C). When the dissolution reactions are included, a good match is obtained with a Q_v value of 0.062 mequiv/mL, which indicates that the CEC remains constant when the temperature increases from 20 to 60 °C.

4.4. Exps. 4−6: Cation Exchange in the Presence of Oil.

To examine the effect of oil saturation on the cation exchange, we performed three two-phase flow experiments (Exps. 4−6). In Exp. 4, we used crude oil type A (high base/acid ratio) without aging the rock. Using the same core we performed experiment (4a) at 20 °C and (4b) at 60 °C. In Exp. 5 and Exp. 6, we used crude oil type B (low base/acid ratio) and the experiments were both performed at 60 °C. The core was aged in Exp. 6 whereas in Exp. 5 the core was not aged.

Figure 8 shows the effluent ion concentrations as a function of the injected pore volumes of low-salinity brine at a "remaining" oil saturation of S_{orem} = 0.45 ± 0.03 and T = 20 °C (Exp. 4a). During the low-salinity water injection, about 2% of the oil initially in place (OIIP) was produced. In view of this small oil production, we assume that the oil saturation remains more or less unchanged and that the PHREEQC solution for a single aqueous phase flow problem can be applied for the interpretation where we assume interaction with a stationary adsorber. With these assumptions, the PHREEQC solution provides a reasonable match with the measured data at 20 °C. We used a Q_v and dispersivity-length values of 0.055 mequiv/mL and 0.85 cm to optimize agreement between the experiment and PHREEQC results. These values are close to the values obtained from the oil-free experiment shown in Figure 6. However, the small reduction of the Q_v value from 0.062 mequiv/mL to 0.055 mequiv/mL is related to differences in the rock mineralogy and not to the presence of oil, as we will notice in Exp. 6b.

Exp. 4b was conducted after conducting Exp. 4a. In this experiment, HSB was injected to the core at T = 60 °C to establish the same initial condition as for Exp. 4a. Next, LSB was injected into the core. When the temperature is increased

DOI: 10.1021/acsearthspacechem.6b00015
ACS Earth Space Chem. 2017, 1, 101−112

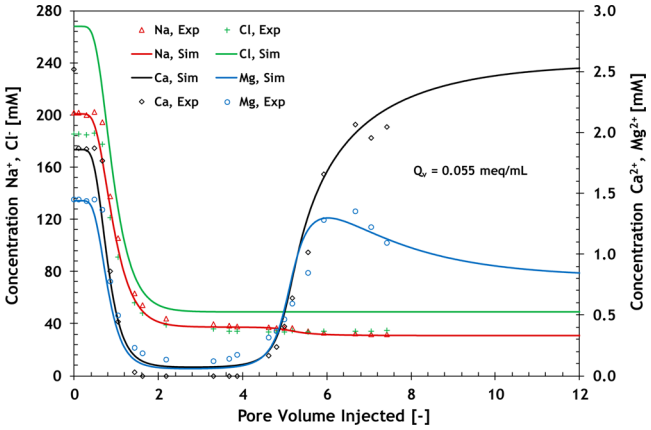

Figure 8. History of concentrations of effluent ions in Exp. 4a with crude oil type A (high base/acid ratio) at T = 20 °C and S_{orem} = 0.45 ± 0.03. The core was not aged with the crude oil. Symbols indicate measured concentration, lines are modeled.

to 60 °C (Exp. 4b), the behavior was different. Indeed, with the increase of temperature from 20 to 60 °C more oil was produced due to the reduction of oil viscosity or its expansion, which resulted in a remaining oil saturation of S_{orem} = 0.40 ± 0.03. The results of this experiment and the model results for various Q_v results are shown in Figures 9 and 10.

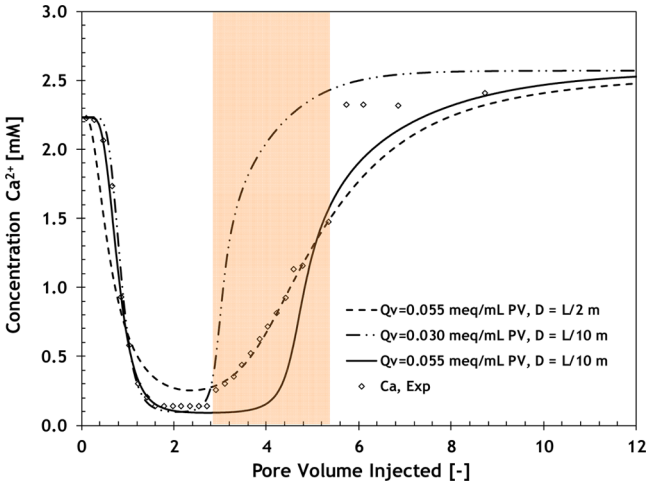

Figure 9. History of concentrations of effluent ions in Exp. 4b with crude oil type A (high base/acid ratio) at T = 60 °C and S_{orem} = 0.40 ± 0.03. The core was not aged with the crude oil. Symbols indicate measured concentration, lines are modeled.

It is more difficult to interpret the results because the third region (rarefaction wave) is more spread out than in the low-temperature case. It appears that now the CEC (represented by Q_v) has decreased; if we assume the same CEC value as in Exp. 4a at 20 °C (Figure 8), there is a clear discrepancy between the experimental and the model results. The solid line in Figure 10 is calculated assuming a CEC value of Q_v = 0.055 mequiv/mL and a dispersivity length of 0.85 cm. By reducing the value of CEC to Q_v = 0.03 mequiv/mL and keeping the same dispersivity value we obtain the broken line in Figure 10, which does not agree well with the experimental data in the third region of the cation exchange process. A good agreement is obtained with a CEC value of Q_v = 0.055 mequiv/mL and a dispersivity length of 8.5 cm (see also Figure 10). Even if the

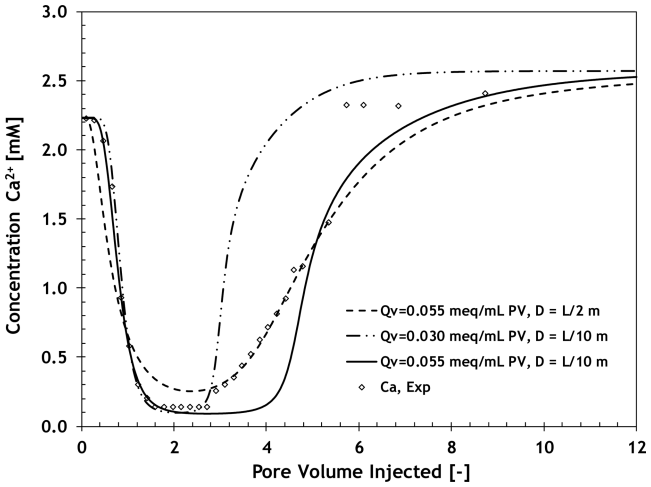

Figure 10. History of concentration of Ca^{2+} in Exp. 4b with crude oil type A (high base/acid ratio) at T = 60 °C and S_{orem} = 0.40 ± 0.03. The core was not aged with the crude oil. The lines present simulations using different assumptions on CEC and the dispersivity length. D denotes the dispersivity length and L is the length of the core.

presence of oil could enhance the dispersion considerably in porous media,[18,67] the increase of dispersivity by a factor of 10 was not inferred from experiments 5 and 6 conducted on a similar Berea sandstone core.

The conventional concept that determines the wetting effects is as follows: when the charges at the oil−water interface have the same sign as the charges of the rock−water interface it is possible to have a macroscopic water film and typical water-wet behavior. Repulsive forces originate from the double layers at the oil−water and rock−water surfaces. The repulsive forces become less at high ionic strength, which shields the surface charge. van der Waals forces with a layer of high dielectric coefficient and low refractive index (water) between the rock and the oleic phase are always attractive (see ref 29). These forces lead together to the disjoining pressure. If the capillary pressure exceeds the maximum disjoining pressure of the thick water film, then thick water film becomes unstable. When the double layers have opposite signs it is unlikely that a thick water film is stable. In the absence of a macroscopic water film, the rock becomes hydrophobic. At short ranges, the structural forces and the hydrogen bonding must be considered. The Pauli Exclusion Principle leads to repulsion between surfaces at extremely close range. For our interpretation, we refer to Figure 11 in which we extend this conceptual picture in case of highly irregular pore surfaces (more the rule than the exception) and to accommodate the presence of clays, which have both positively- and negatively charged sites. Figures 1 and 11 give a schematic picture of an oil ganglion inside a pore with a highly irregular surface. The conventional division between completely oil-wet or water-wet surfaces is modified as follows. Clay edges and asperities are pinning points for the oil ganglion.[20−22] Some parts of the edges can be negatively charged while other parts can be positively charged. The polar components (negatively charged carboxylic, naphthenic acids and positively charged amines, cationic surfactants, pyridines) with opposite charges are adsorbed to the rock and provide surfaces of low interaction energy with the oil ganglion. Also neutral components (e.g., phenols) can be adsorbed by van der Waals forces and ligand bonding and thus create oil-wet spots. Other parts of the rock carry a water film with a thickness of the

DOI: 10.1021/acsearthspacechem.6b00015
ACS Earth Space Chem. 2017, 1, 101−112

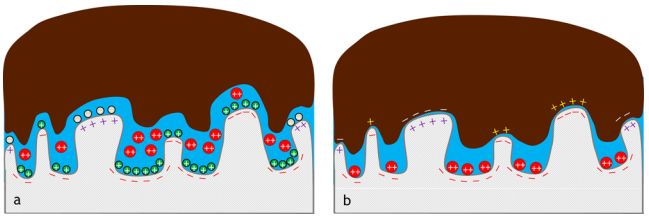

Figure 11. Schematic of cation exchange involving both inorganic species and oil. (a) Just before the exchange between the oil, brine, and rock starts; (b) after enough time is given for oil to interact. For simplicity, the solution ions in image (b) are not drawn. Both anion and cation exchange reactions can occur between crude oil and the rock, depending on the composition of the crude oil. The negatively charged sites on the rock surface are mainly clay surface, whereas the positively charged sites could be either clay edges, or Ca- and Mg-containing oxides or minerals such as calcite or dolomite. The rock surface charge has been assumed heterogeneous, that is, both negative and positive charges are considered for clay surfaces.

order of the Debye length, which will be between the rock and oil surface.

Consequently, it can also be argued that presence of oil does not impact the total number of exchangeable sites on the rock surface. Recall that in the PHREEQC calculations, the CEC value is calculated from the width of the region with low concentrations of divalent cations. Nevertheless, when oil is present in the core, it is plausible that there is multicomponent adsorption of ions (on the rock surface or oil surface) involving both inorganic species (Na^+, Ca^{2+}, Mg^{2+}) and polar compounds in the crude oil, as shown in Figure 11. It appears that these reactions are kinetically controlled and the polar components of the crude oil become more active at higher temperatures.[26,68] Referring to Figure 11, the geochemical reactions, including cation exchange reactions, occur within the water films. Therefore, the presence of an (inert) oil drop is not expected to influence the final composition of the aqueous phase, although the transport of the ions from (and toward) this film to the bulk brine may be impeded. However, slow mass transfer should affect the whole length of the intermediate stripped region with low divalent-cation concentration (region 2), which is not observed in the results shown in Figures 9 and 10. Instead, it is likely that the polar components such as naphthenic acids, cationic surfactants, and pyridine molecules (base components) are attracted to the surface of the clay minerals with an opposite charge. The positively (negatively) charged compounds such as pyridine (carboxylic or naphthenic acids) can adsorb directly onto the rock surface at negatively (positively) charged pinning points (asperities or edges), albeit in the presence of a very thin water film because the polar functional groups accumulate at the oil/brine interface.[29,69] The higher Ca^{2+} and Mg^{2+} concentrations in the shaded area compared to the calculated equilibrium curve from PHREEQC in Figures 9 and 10 are attributed to higher amounts of basic or positively charged species in the crude oil compared to the acidic compounds. In other words, the higher concentrations of the divalent cations are because of the exchange with the positively charged species in the oil. Attachment of acidic or negatively charged components can also occur due to cation bridging or ligand bonding, which strips away exchangeable cations from the bulk aqueous solution.

The total surface of the clay minerals is a sum of external (edge) and internal (basal or faces) surfaces (for the terminologies see Table 4). Both surfaces carry charges; however, the origin of the charge on these surfaces is different. The charges on the external surfaces are pH-dependent and originate from the −OH sites on the (broken) edges of crystal lattices.[39] The charges in the internal surfaces are result of the isomorphic substitution of the ions, that is, a cation with a larger charge (tetra- or trivalent) is substituted by a cation with a smaller charge (tri- or bivalent) resulting in a negative charge. Therefore, in 2:1 clays the interlayer space can accumulate hydrated or dehydrated cations to neutralize the negative charge. In clays like kaolinite, the pH-dependent charges contribute to the major proportion of the total net charge. On the contrary, the charges in internal surface contribute to more than 85% of the total charge of the 2:1 clays like vermiculite, smectite, and chlorite.[37−39] The first part of the stripped region in Figures 9 and 10 is mainly attributed to cation exchange of the injected brine with the cations residing in the internal surface of the clays (permanent sites). Adsorption of the charged components of the crude oil is therefore expected to occur on the broken edges (with pH-dependent charges) or positively charged minerals such as calcite and dolomite at neutral pH values.

4.5. Exp. 5: Effect of Type of Crude Oil. In order to investigate the effect of the type of crude oil, Exp. 5 was performed at 60 °C and with crude oil type B (low base/acid ratio), which contains less basic compounds compared to crude oil type A (high base/acid ratio) (Table 2). Figures 12 and 13

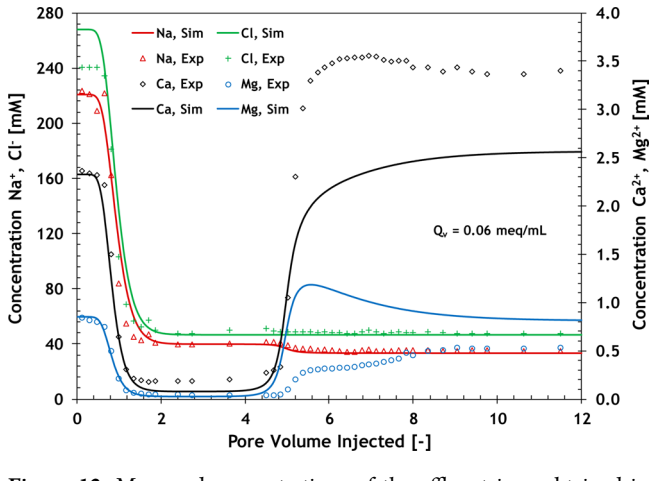

Figure 12. Measured concentrations of the effluent ions obtained in Exp. 5a at T = 60 °C. No oil was present in the core.

show the history of the measured ions at the core outlet during single-phase (Exp. 5a) and two-phase stages (Exp. 5b) of the experiment, respectively. It appears that in both stages the measured values of Ca^{2+} and Mg^{2+} ions are higher than the initial and injected values of the ions, which is attributed to dissolution of Ca- and Mg-containing minerals in the rock. When oil is present after the retardation front, the behavior of $Ca^{2+}$and Mg^{2+} suggests another exchange between $Ca^{2+}$and Mg^{2+}, where the concentration of Mg^{2+} is lower and Ca^{2+} is higher than the equilibrium concentration. The core we used in Exp. 5 was not from the same block as used in the other experiments. The difference might result from the different mineralogy of the rock. Nevertheless, the CEC value (0.06 mequiv/mL) is the same as in other experiments by fitting two fronts. The history of ions in Exp. 5b exhibits a similar behavior as in Exp. 4b, that is, between the two fronts there exists a region with a low concentration of the divalent ions and a region in which concentration of Ca^{2+} and Mg^{2+} gradually rise to the injected concentrations. Comparing the

DOI: 10.1021/acsearthspacechem.6b00015
ACS Earth Space Chem. 2017, 1, 101−112

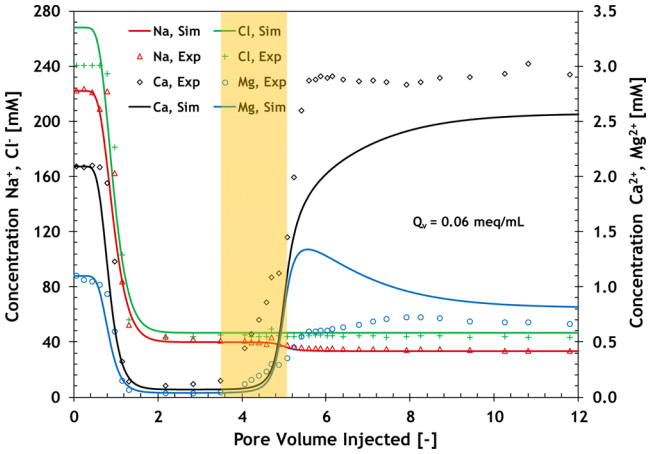

Figure 13. Measured concentrations of each ion obtained Exp. 5b containing remaining crude oil type B (low base/acid ratio, S_{orem} =0 .40 ± 0.03). T = 60 °C. The core was not aged with the crude oil.

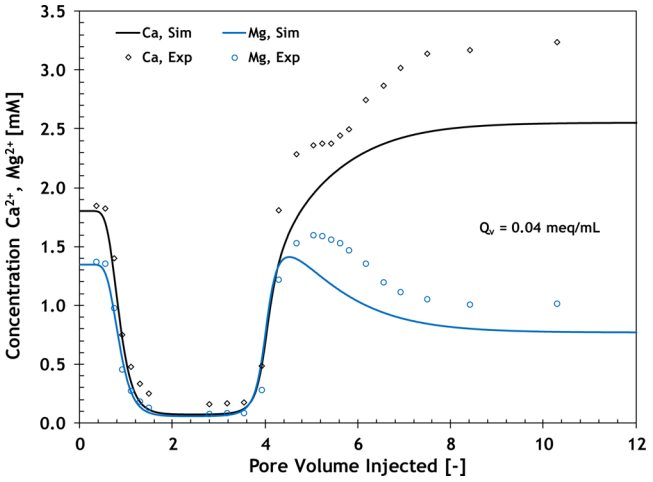

Figure 14. PHREEQC model (lines) and measured concentrations of cations obtained in during single-phase stage of the experiment, Exp 6a at T = 60 °C.

shaded areas in Figures 10 and 13 reveals that the length of the transition zone in Exp. 4b is longer than in Exp. 5b. This is because of the difference in net charges of the two oil types. The base/acid ratio of oil type A is higher than that of the oil type B (low base/acid ratio). This again confirms that the base or positively charged components of the oil compete with the divalent ions for the negatively charged sites on clays minerals. Our results are consistent with the finding that polar oil components are adsorbed more on rock for crude oils with a high base/acid ratio,[70,71] which is attributed to the adsorption of the base components to the negative sites of the rock.[28,29,31]

Furthermore, after the second front the concentration of Ca^{2+} in the single-phase stage of the experiment (Figure 12) is higher than that of the two-phase stage (Figure 13). This suggests that when oil is present in the porous medium, less calcite is dissolved because the negatively charged components cover the calcite and dolomite surfaces. In the pH range of our experiments, calcite and dolomite surfaces are positively charged[32−34,72] and therefore the negatively charged components of the crude oil can adsorb on the calcite surface and inhibit or delay the dissolution process.

4.6. Exp. 6: Effect of Aging. In Exp. Four and Exp. Five, the core was directly flushed with the high-salinity brine after saturating the core with oil, that is, there was not ample time for the oil and the rock to interact. In Exp. 6, after the single-phase stage, the core was resaturated with the high-salinity brine. Afterward, the core was saturated with crude oil type B (low base/acid ratio) and the setup was shut down for 8 weeks at constant pressure (50 bars) and temperature of 60 °C to allow time for the minerals and the fluids to interact and alter the rock wettability toward nonwater wet conditions. Under these conditions, the water film covering the surface can be very thin or unstable and therefore the polar components in the crude oil can directly adsorb onto the rock surface[73] (see Figure 11). The low-salinity brine was then injected to study the effect of wetting behavior of the rock surface upon cation exchange.

Figure 14 shows the history of the ion concentrations of the single-phase stage of the experiment. The CEC of this core was calculated to be Q_v = 0.04 mequiv/mL, which is lower than that of the core used in the previous experiments. Also the high concentrations of Ca^{2+} and Mg^{2+} at the later stages of the experiment suggest dissolution of calcite and dolomite. The results of the two-phase stage (Exp. 6b) of this experiment, shown in Figure 15, reveal some remarkable differences compared to Exp. 4b (Figure 9) and Exp. 5b (Figure 13). The

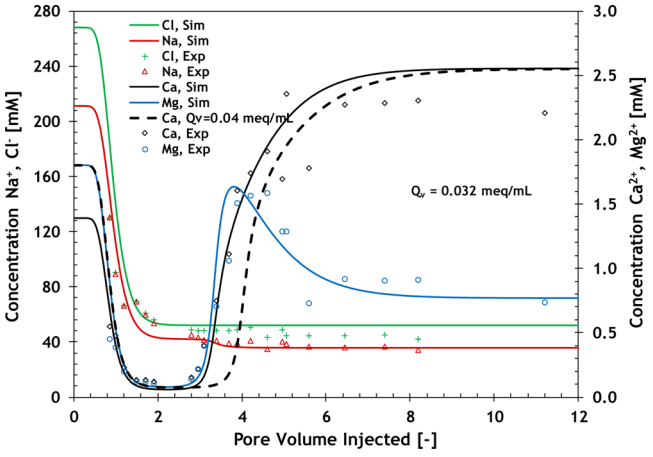

Figure 15. PHREEQC model (lines) and measured concentrations of each ion obtained in the experiment with immobile crude oil B (low base/acid ratio), Exp 6b at T = 60 °C. The core was aged with the core.

transition region observed in Exp. 4b and Exp. 5b has disappeared in Exp. 6b and only a region with constant low concentrations of divalent cations exists between the two fronts. The experimental data can be simulated using a CEC value of Q_v = 0.032 mequiv/mL, which is about 20% smaller than the CEC of the single-phase stage of the experiment, that is, Exp. 6a (Figure 14). The dashed line in Figure 15, calculated using the CEC value of Exp. 6a (Q_v = 0.04 mequiv/mL), deviates from the experimental data. Finally, dissolution of the minerals (calcite or dolomite) can no longer be inferred from the data.

It can be inferred from our experimental data that when there is enough time between the oil and the rock to interact, the positively (negatively) charged components of the crude oil are fully attracted to the rock to neutralize the negatively (positively) charged sites of the rock. In contrast to the water-wet surfaces, the cation bridging of the oil with the rock appears to be less important for the nonwater-wet spots because of their weak nature. Consequently, it is less likely that oil can be desorbed from the rock surface because of multicomponent cation exchange between the aqueous phase and the clays. Furthermore, the acidic

DOI: 10.1021/acsearthspacechem.6b00015
ACS Earth Space Chem. 2017, 1, 101−112

or negatively charged components of the crude oil cover the positively charged calcite and dolomite sites and prevent the rock dissolution. The extent of these multicomponent exchanges depends on the oil, brine, and rock compositions.

5. CONCLUSIONS

Under our experimental conditions (rock type and composition, brine compositions, oil types, and so forth) the following conclusions can be drawn from this study:

- Cation exchange is a reversible process at the salinity range we probed.
- The kinetics effects (nonequilibrium) on the cation exchange in the single-phase flow experiments are insignificant at the range we studied.
- The temperature dependence of the CEC of the Berea sandstone can be disregarded for the temperature range of this study (20−60 °C).
- Inclusion of the dissolution reactions are required to obtain meaningful information on the CEC when experiments at different temperatures are compared.
- In the presence of crude oil, base components of the oil participate in the cation exchange process. In this case, the ion exchange is a kinetically controlled process and its rate depends on residence time of oil in the pore, temperature, and kinetics rate of adsorption of the polar groups on the rock surface.
- At low temperatures (e.g., at room temperature), the exchange of ions between crude oil and the surrounding rock surface can be neglected, that is, all available sites exchange ions exclusively with the aqueous phase.
- The cation-exchange process occurs in two stages during two-phase flow in porous media. Initially, the charged sites of the internal surface of the clays establish a new equilibrium by exchanging cations with the aqueous phase. At later stages, the components of the aqueous and oleic phases compete for the charged sites on the external surface or edges of the clays.
- When there is sufficient time for crude oil to interact with the rock (i.e., when core is aged with crude oil), a fraction of the charged sites are neutralized by the charged components stemming from crude oil. This suggests that the apparent cation exchange capacity of rock decreases in the presence of crude oil.
- The positively charged calcite and dolomite surfaces (at the pH conditions of our experiments) are covered with the negatively charged components of the crude oil and therefore less or no dissolution takes place when oil is present in porous media.

APPENDIX A

Figures A.1 and A.2 are shown below:

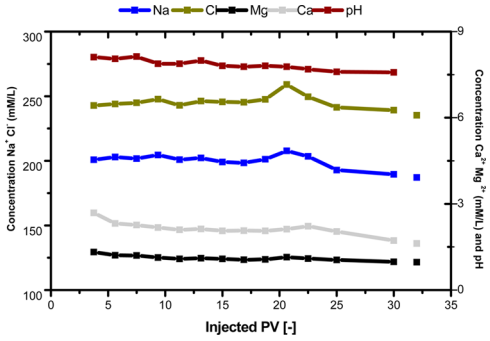

Figure A.1. Production profile of effluents obtained from the ICP measurement and pH value during high-salinity brine injection.

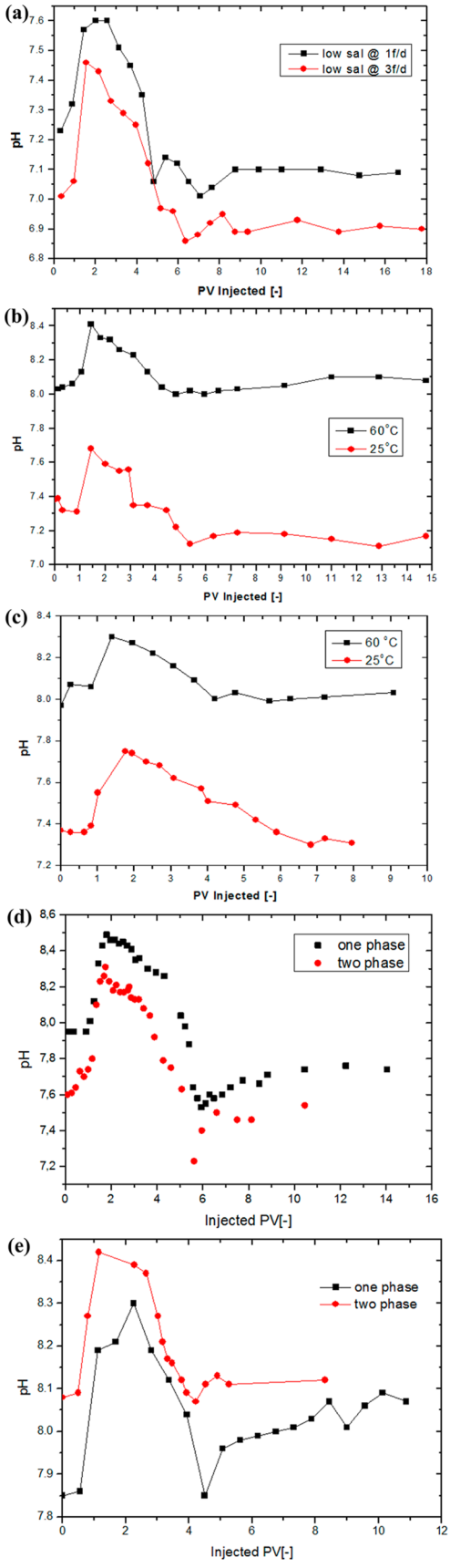

Figure A.2. History of the effluent pH values: (a) Exp. 2, (b) Exp. 3, (c) Exp. 4, (d) Exp. (5), and (e) Exp. 6.

DOI: 10.1021/acsearthspacechem.6b00015
ACS Earth Space Chem. 2017, 1, 101−112

AUTHOR INFORMATION

Corresponding Author

*E-mail: R.Farajzadeh@tudelft.nl.

ORCID

R. Farajzadeh: 0000-0003-3497-0526

Notes

The authors declare no competing financial interest.

ACKNOWLEDGMENTS

The authors are grateful to Steffen Berg, Ramez Nasralla, Hassan Mahani, and Ali Fadili for the fruitful discussions and valuable comments on the draft of the manuscript. Shell Global Solutions International is also acknowledged for granting permission to publish this work.

REFERENCES

(1) Lake, L.; Johns, R.; Rossen, W. R.; Pope, G. *Fundamentals of Enhanced Oil Recovery*; Society of Petroleum Engineers, 2014.

(2) Lotfollahi, M.; Farajzadeh, R.; Delshad, M.; Al-Abri, A.-K.; Wassing, B. M.; Al Mjeni, R.; Awan, K.; Bedrikovetsky, P. Mechanistic Simulation of Polymer Injectivity in Field Tests. *SPE J.* **2016**, *21* (04), 1178−1191.

(3) Tang, G. Q.; Morrow, N. R. Influence of brine composition and fine migration on crude oil/brine/rock interactions and oil recovery. *J. Pet. Sci. Eng.* **1999**, *24*, 99−111.

(4) Tang, G. Q.; Morrow, N. R. Salinity, temperature, oil composition and oil recovery by waterflooding. *SPE Reservoir Eng.* **1997**, *12* (04), 269.

(5) Austad, T.; RezaeiDoust, A.; Puntervold, T. *Chemical Mechanism of Low Salinity Water Flooding in Sandstone Reservoirs*. SPE 129767. Society of Petroleum Engineers: Tulsa, OK, 2010.

(6) RezaeiDoust, A.; Puntervold, T.; Austad, T. Chemical Verification of the EOR Mechanism by Using Low Saline/Smart Water in Sandstone. *Energy Fuels* **2011**, *25* (5), 2151−2162.

(7) Lager, A.; Webb, K. J.; Black, C. J.; Singleton, M.; Sorbie, K. S. Low Salinity Oil Recovery: An Experimental Investigation. *Petrophysics* **2008**, *49* (1), 28−35.

(8) Mahani, H.; Berg, S.; Ilic, D.; Bartels, W. B.; Joekar-Niasar, V. Kinetics of low-salinity-flooding effect. *SPE J.* **2015**, *20* (01), 008−020.

(9) Joekar-Niasar, V.; Mahani, H. Nonmonotonic Pressure Field Induced by Ionic Diffusion in Charged Thin Films. *Ind. Eng. Chem. Res.* **2016**, *55* (21), 6227−6235.

(10) Mahani, H.; Sorop, T.; Ligthelm, D. J.; Brooks, D.; Vledder, P.; Mozahem, F.; Ali, Y. *Analysis of field responses to low-salinity waterflooding in secondary and tertiary mode in Syria*. SPE 142960, SPE EUROPEC/EAGE Annual Conference and Exhibition. Society of Petroleum Engineers: Tulsa, OK, 2011.

(11) Mahani, H.; Keya, A. L.; Berg, S.; Nasralla, R. Electrokinetics of Carbonate/Brine Interface in Low-Salinity Waterflooding: Effect of Brine Salinity, Composition, Rock Type, and pH on ζ-Potential and a Surface-Complexation Model. *SPE J.* **2017**, *22* (01), 053−068.

(12) Nasralla, R. A.; Nasr-El-Din, H. A. Double-layer expansion: is it a primary mechanism of improved oil recovery by low-salinity waterflooding? *SPE Reservoir Eval. .Eng.* **2014**, *17*, 49−59.

(13) Nasralla, R. A., Snippe, J. R.; Farajzadeh, R. *Coupled Geochemical-Reservoir Model to Understand the Interaction Between Low Salinity Brines and Carbonate Rock*. SPE 174661, SPE Asia Pacific Enhanced Oil Recovery Conference. Society of Petroleum Engineers: Tulsa, OK, 2015.

(14) Borazjani, S.; Behr, A.; Genolet, L.; Van Der Net, A.; Bedrikovetsky, P. Effects of Fines Migration on Low-Salinity Waterflooding: Analytical Modelling. *Transp. Porous Media* **2017**, *116*, 213−249.

(15) Borazjani, S.; Bedrikovetsky, P.; Farajzadeh, R. Analytical solutions of oil displacement by a polymer slug with varying salinity. *J. Pet. Sci. Eng.* **2016**, *140*, 28−40.

(16) Zeinijahromi, A.; Nguyen, T. K. P.; Bedrikovetsky, P. Mathematical model for fines-migration-assisted waterflooding with induced formation damage. *SPE J.* **2013**, *18* (03), 518−533.

(17) Zeinijahromi, A.; Farajzadeh, R.; Bruining, J.; Bedrikovetsky, P. Effect of fines migration on oil−water relative permeability during two-phase flow in porous media. *Fuel* **2016**, *176*, 222−236.

(18) Karadimitriou, N. K.; Joekar-Niasar, V.; Babaei, M.; Shore, C. A. Critical Role of the Immobile Zone in Non-Fickian Two-Phase Transport: A New Paradigm. *Environ. Sci. Technol.* **2016**, *50* (8), 4384−4392.

(19) Pathak, P.; Davis, H. T.; Scriven, L. E. *Dependence of residual nonwetting liquid on pore topology*. SPE 11016. 57th Annual Fall Technical Confenrence and Exhibition of SPE of AIME; New Orleans, LA, Sept. 26−29, 1982.

(20) Schmatz, J.; Urai, J. L.; Berg, S.; Ott, H. Nano-scale Imaging of Pore-scale Fluid-Fluid-Solid Contacts in Sandstone. *Geophys. Res. Lett.* **2015**, *42* (7), 2189−2195.

(21) Salathiel, R. Oil recovery by surface film drainage in mixed-wettability rocks. *JPT, J. Pet. Technol.* **1973**, *25*, 1216−1224.

(22) Morrow, N. R.; Lim, H. T.; Ward, J. S. Effect of crude oil-induced wettability changes on oil recovery. *SPE Form. Eval.* **1986**, *1*, 89−103.

(23) Brady, P. V.; Morrow, N. R.; Fogden, A.; Deniz, V.; Loahardjo, N. Winoto. Electrostatics and the low salinity effect in sandstone reservoirs. *Energy Fuels* **2015**, *29*, 666−677.

(24) Morrow, N. R. Wettability and its effect on oil recovery. *JPT, J. Pet. Technol.* **1990**, *42*, 1476−1484.

(25) Buckley, J. S.; Takamura, K.; Morrow, N. R. Influence of electrical surface charges on the wetting properties of crude oils. *SPE Reservoir Eng.* **1989**, *4*, 332−340.

(26) Villard, J.-M.; Buckley, J.; Morrow, N.; Gauchet. Wetting and waterflood oil recovery of a moderately viscous oil. SCA Conference paper number 9323, 1993.

(27) Buckley, J. S.; Morrow, N. R. *Characterization of crude oil wetting behavior by adhesion tests*. SPE 20263. 7th Symposium on Enhanced Oil recovery, Tulsa, OK, 1990.

(28) Dubey, S. T.; Doe, P. H. Base number and wetting properties of crude oils. *SPE Reservoir Eng.* **1993**, *8*, 195−200.

(29) Hirasaki, G. J. Wettability: Fundamentals and Surface Forces. *SPE Form. Eval.* **1991**, *6* (02), 217−226.

(30) Hirasaki, G. J. Structural interactions in the wetting and spreading of Van der Waals fluids. *J. Adhes. Sci. Technol.* **1993**, *7* (3), 285−322.

(31) Israelachvili, J. N. *Intermolecular and Surface Forces*, 3rd ed.; Academic Press, 1991.

(32) Brady, P.; Krumhansl, J. L. A surface complexation model of oil-brine-sandstone interfaces at 100C: Low salinity waterflooding. *J. Pet. Sci. Eng.* **2012**, *81*, 171−176.

(33) Brady, P. V.; Randall, C. T.; Nagy, K. L. Molecular controls on kaolinite surface charge. *J. Colloid Interface Sci.* **1996**, *183* (2), 356−364.

(34) Brady, P.; Krumhansl, J. L.; Mariner, P. E. *Surface Complexation Modeling for Improved Oil Recovery*. SPE 153744, SPE Improved Oil Recovery Symposium, Tulsa, OK, April 14−18, 2012.

(35) Parkhurst, D. L.; Appelo, C. A. J. User's guide to PHREEQC (Version 2)-A Computer program for speciation, batch-reaction, one-dimensional transport, and inverse geochemical calculations. Water-resources investigations Report 99-4259, U.S. Geological Survey: Denver, CO, http//wwwbrr.cr.usgs.gov/projects/GWC_coupled/phreeqc/index.html.

(36) Sposito, G. *The chemistry of soils*; Oxford University Press, 1989.

(37) Stumm, W.; Morgan, J. J. *Aquatic chemistry Chemical Equilibria and Rates in Natural Waters*, 3rd ed.; Wiley Interscience, 1995.

(38) McBride, M. B. *Environmental Chemistry of Soils*; Oxford University Press, 1994.

(39) Nagy, N. M.; Konya, J. *Interfacial Chemistry of Rocks and Soils*; CRC Press, 2010.

DOI: 10.1021/acsearthspacechem.6b00015
ACS Earth Space Chem. 2017, 1, 101−112

(40) Appelo, C. A. J. Cation and proton exchange, pH variation, and carbonate reactions in a freshening aquifer. *Water Resour. Res.* **1994**, *30*, 2793−2805.
(41) Appelo, C. A. J.; Postma, D. *Geochemistry, groundwater and pollution*, 2nd ed.; A.A. Balkema Publishers: Leiden, 2005.
(42) Valocchi, J.; Roberts, P. V.; Parks, G. A.; Street, R. L. Simulation of the transport of ion exchanging solutes using laboratory-determined chemical parameter values. *Groundwater* **1981**, *19* (6), 600−607.
(43) Pope, G. A.; Lake, L. W. Cation exchange in chemical flooding: Part 1- Basic theory without dispersion. *SPEJ, Soc. Pet. Eng. J.* **1978**, *18* (06), 418−434.
(44) Lake, L. W.; Helfferich, F. Cation exchange in chemical flooding: Part 2- the effect of dispersion, cation exchange, and polymer/surfactant adsorption on chemical flood environment. *SPEJ, Soc. Pet. Eng. J.* **1978**, *18* (06), 435−444.
(45) Hill, H. J.; Lake, L. W. Cation exchange in chemical flooding: Part 3 − Experimental. *SPEJ, Soc. Pet. Eng. J.* **1978**, *18* (06), 445−456.
(46) Hirasaki, G. J. Ion exchange with clays in the presence of surfactant. *SPEJ, Soc. Pet. Eng. J.* **1982**, *22* (02), 181−192.
(47) Farajzadeh, R.; Matsuura, T.; van Batenburg, D.; Dijk, H. Detailed modeling of the alkali/surfactant/polymer (ASP) process by coupling a multipurpose reservoir simulator to the chemistry package PHREEQC. *SPE Res. Eval. Eng.* **2012**, *15* (4), 423−435.
(48) Bunge, A. L.; Radke, C. J. Divalent Ion Exchange With Alkali. *SPEJ, Soc. Pet. Eng. J.* **1983**, *23* (4), 657−668.
(49) Bhuyan, D.; Lake, L. W.; Pope, G. A. Mathematical Modeling of High-pH Chemical Flooding. *SPE Reservoir Eng.* **1990**, *5* (2), 213−220.
(50) Delshad, M.; Pope, G. A.; Sepehrnoori, K. *Vol. II: Technical Documentation for UTCHEM-9.0, A Three-Dimensional Chemical Flood Simulator*; Technical Documentation, Center for Petroleum and GeosystemsEngineering; The University of Texas at Austin: Austin, TX, 2000. http://www.cpge.utexas.edu/sites/default/files/research/UTCHEM_Tech_Doc.pdf (accessed March 14, 2017).
(51) Mohammadi, H.; Delshad, M.; Pope, G. A. Mechanistic Modeling of Alkaline/Surfactant/Polymer Floods. *SPE Res. Eval. Eng.* **2009**, *12* (04), 518−527.
(52) Regtien, J. M. M.; Por, G. J. A.; van Stiphout, M. T.; van der Vlugt, F. F. *Interactive Reservoir Simulation*. Paper SPE 29146 presented at theSPE Reservoir Simulation Symposium, San Antonio, Texas, February 12−15, 1990.
(53) Wei, L. *Rigorous Water Chemistry Modelling in Reservoir Simulationsfor Waterflood and EOR Studies*. Paper SPE 138037 presented at the Abu DhabiInternational Petroleum Exhibition and Conference, Abu Dhabi, UAE, November 1−4, 2010.
(54) van Bladel, R.; Gheyi, H. R. Thermodynamics study of calcium-sodium and calcium-magnesium exchange in calcareous soils. *Soil Sci. Soc. Am. J.* **1980**, *44* (5), 938−942.
(55) Laudelout, H.; van Bladel, R.; Bolt, G. H.; Page, A. L. Thermodynamics of heterovalent cation exchange reactions in a montmorillonite clay. *Trans. Faraday Soc.* **1968**, *64*, 1477−1488.
(56) Churcher, P. L.; French, P. R.; Shaw, J. C.; Schramm, L. L. *Rock properties of Berea sandstone, Baker dolomite, and Indiana limestone*. SPE International Symposium on Oilfield Chemistry, February 20−22, 1991.
(57) Ramirez, W. F.; Oen, A. C.; Strobel, J. F.; Falconer, J. L.; Evans, H. E. Surface composition of Berea sandstone. *SPE Form. Eval.* **1986**, *1* (1), 23−30.
(58) Nguyen, Q. P.; Currie, P. K.; Buijse, M.; Zitha, P. L. J. Mapping of foam mobility in porous media. *J. Pet. Sci. Eng.* **2007**, *58*, 119−132.
(59) Andrianov, A.; Farajzadeh, R.; Mahmoodi Nick, M.; Talanana, M.; Zitha, P. L. J. Immiscible foam for enhancing oil recovery: bulk and porous media experiments. *Ind. Eng. Chem. Res.* **2012**, *51* (5), 2214−2226.
(60) Simjoo, M.; Dong, Y.; Andrianov, A.; Talanana, M.; Zitha, P. L. J. Novel insight into foam mobility control. *SPE J.* **2013**, *18* (03), 416−427.
(61) Zhou, Z.; Gunter, W. D. The nature of the surface charge of Kaolinite. *Clays Clay Miner.* **1992**, *40* (3), 365−368.
(62) Griffioen, J. Multicomponent cation exchange including alkalinization/acidification following flow through sandy sediment. *Water Resour. Res.* **1993**, *29*, 3005−3019.
(63) Griffioen, J.; Anthony, C.; Appelo, J. Nature and extent of carbonate precipitation during aquifer thermal energy storage. *Appl. Geochem.* **1993**, *8* (2), 161−176.
(64) Tewar, P. H.; Lee, W. Adsorption of Co(II) at the oxide-water interface. *J. Colloid Interface Sci.* **1975**, *52*, 77−88.
(65) Johnson, B. B. Effect of pH, temperature, and concentration on the adsorption of cadmium on goethite. *Environ. Sci. Technol.* **1990**, *24* (10), 112−118.
(66) Reppert, P. M.; Morgan, F. D. Temperature-dependent streaming potentials: 2. Laboratory. *J. Geophys. Res.* **2003**, *108* (B11), 2547.
(67) Delshad, M.; MacAllister, D. J.; Pope, G. A.; Rouse, B. A. Multiphase dispersion and relative permeability experiments. *SPEJ, Soc. Pet. Eng. J.* **1985**, *25* (4), 524−534.
(68) Yu, L.; Buckley, J. S. Evolution of Wetting Alteration by Adsorption from Crude Oil. *SPE Form. Eval.* **1997**, *12*, 5−11.
(69) Buckley, J. S.; Liu, Y.; Monsterleet, S. Mechanisms of Wetting Alteration by Crude Oils. *SPE J.* **1998**, *3* (01), 54−61.
(70) Skauge, A.; Standal, S.; Boe, S. O.; Skauge, T.; Blokhus, A. M. *Effect of organic acids and bases, and oil composition on wettability*. SPE 56673. SPE Annual Technical Conference and Exhibition, Houston, TX, October 3−6, 1999.
(71) Buckley, J. S.; Takamura, K. Influence of electrical surface charges on the wetting properties of crude oil. *SPE Reservoir Eng.* **1989**, *4*, 332−340.
(72) Thomas, M. M.; Clouse, J. A.; Longo, J. M. Adsorption of organic compounds on carbonate minerals. 1. Model compounds and their influence on mineral wettability. *Chem. Geol.* **1993**, *109*, 201−213.
(73) Nourani, M.; Tichelkamp, T.; Gawel, B.; Oye, G. Desorption of crude oil components from silica and aluminosilicate surfaces upon exposure to aqueous low salinity and surfactant solutions. *Fuel* **2016**, *180*, 1−8.

DOI: 10.1021/acsearthspacechem.6b00015
ACS Earth Space Chem. 2017, 1, 101−112